Tetrahedron Letters 50 (2009) 1906–1910

Contents lists available at ScienceDirect

Tetrahedron Letters

journal homepage: www.elsevier.com/locate/tetlet

Heterocyclic columnar hexacatenar bisthiazoles

Hui-Hsu Gavin Tsai [a], Lung-Chun Chou [a], Sheng-Chia Lin [a], Hwo-Shuenn Sheu [b], Chung K. Lai [a,*]

[a] Department of Chemistry, National Central University, Chung-Li 32001, Taiwan, ROC
[b] National Synchrotron Radiation Research Center, Hsinchu 30077, Taiwan, ROC

ARTICLE INFO

Article history:
Received 22 November 2008
Revised 1 February 2009
Accepted 3 February 2009
Available online 14 February 2009

Keywords:
Columnar
Hexacatenar
Bisthiazoles
Bisoxazoles

ABSTRACT

Three new series of hexacatenar liquid crystals derived from heterocyclic bisthiazoles and bisoxazoles exhibiting columnar phases were reported, and the formation of columnar phases was strongly sensitive to central heteroatoms and/or their positions incorporated.

Polycatenar liquid crystals,[1] represented as a new structural motif in exploring new mesogenic materials, have been extensively investigated during the past decades. The general structures of such mesogens[2] are virtually based on calamitic molecules, and often constituted by a relatively long central aromatic core surrounded by more-than-two terminal aliphatic chains on both ends. The core structures of known examples are composed of rigid elongated polyaromatic[1b] or highly conjugated heterocyclic-fused rings (1,3,4-oxadiazole,[1a] oxazolines,[1h] bipyridine[2a,3]). On the other hand, the overall molecular shapes are more likely considered as lath-like, that is, between rod- and disc-shaped. A symmetric central core with four and six terminal chains was often applied to generate mesophases. Molecules with four, five, or six terminal chains (i.e., so-called tetra-, penta-, or hexacatenar mesogens[2a]) often preferably gave columnar phases. In a few cases, nematic[1a], smectic,[1a,f] or cubic phases[1f,3a] were occasionally observed for tetracatenar mesogens. A phase crossover[1a,4] between lamellar and columnar phases[4] was also reported. A few interesting examples[1d,5] of columnar phases induced by lyotropic 1*H*-imidazoles was also reported. Some disc-shaped molecules, particularly with an extended conjugated core have emerged as potential electronic materials in technology applications, such as organic field-effect transistors (OFETs) or photovoltaics[6] (OPVs). Interestingly, N, SmC, cubic, and columnar phases in some tetracatenar mesogens[1a,7] were also observed depending on the terminal chain lengths.

On the other hand, efficient light-emitting diode (LED) materials derived from heterocyclic benzoxazoles or benzobisazoles[8a] have been studied. An efficient π-stacking and strong intermolecular interaction[8a] were attributed to some novel physicochemical and mechanical properties observed in such materials. Heterocyclic derivatives were often considered as electron deficient moieties, and an intermolecular dipole was often induced by donor–acceptor (D–A; aromatic as donor, heterocycle as acceptor) interaction when structurally fused to aromatic rings. However, known examples derived from benzobixazoles or benzobisazoles exhibiting mesomorphic behavior were relatively rare. A similar structure of 2,6-bis-(4-[6-(3-ethyl-3-methylene oxyoxetan)hexyl]phenyl)benzo [1,2-d-4,5-d′]-bisthiazole[9] was recently reported, and this compound formed N, and SmA phase. In this work, we describe three new series of hexacatenar bisthiazoles and bisoxazoles exhibiting columnar phases. The formation of columnar phase, Col_h or Col_r phase, was determined or controlled by the heteroatoms and/or the position incorporated.

In order to understand the effect of heteroatoms incorporated on the formation of the mesophases, five derivatives of bisthiazoles **1** (n = 8, 10, 12, 14, 16) were prepared. The synthetic pathways for compounds **1**–**2** are listed in Scheme 1. All compounds were characterized by ^{1}H, ^{13}C NMR spectroscopy, and elemental analysis, and their mesomorphic properties were investigated by differential scanning calorimetry (DSC) and polarizing optical microscopy (POM). The results were compared with those observed by structurally similar bisoxazoles **2** (n = 12).

Under polarized optical microscope, upon heating all materials melt to give birefringent fluid phases with columnar superstructures, and a large area of mosaic textures displaying prominent wedge-shaped defect patterns (Fig. 1) was easily observed. All compounds **1** were then investigated by powder XRD experiments (Fig. 2) at various temperatures to examine their mesophase structures. Rectangular columnar phases[10] often displayed two intense

* Corresponding author. Tel.: +886 03 4259207; fax: +886 03 4277972.
E-mail address: cklai@cc.ncu.edu.tw (C.K. Lai).

0040-4039/$ - see front matter © 2009 Elsevier Ltd. All rights reserved.
doi:10.1016/j.tetlet.2009.02.078

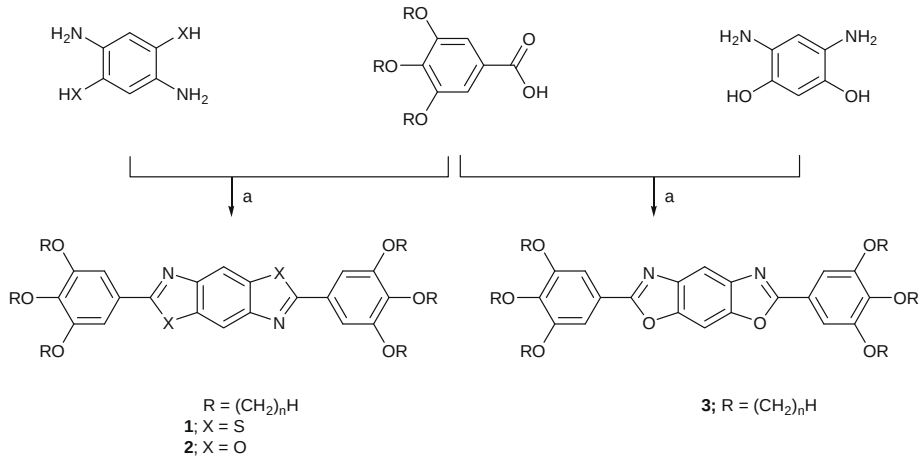

Scheme 1. Reagents and conditions; $SOCl_2$ (1.05 equiv), refluxed in NMP, 48 h, 31–43%.

diffraction peaks in the lower angle region, which were indexed as (2 0 0) and (1 1 0) reflections. For example, the compound **1** (n = 12) gave a diffraction of two strong reflections at d 28.43 Å and 26.13 Å and also a broad diffuse halo peak at d 4.56 Å at 77.0 °C. This diffraction pattern corresponded to rectangular lattice constants: a = 52.26 Å and b = 33.88 Å. In other cases, higher orders of diffraction peaks; $d_{020} \sim 16.89$ Å, $d_{310} \sim 15.42$ Å, and $d_{400} \sim 13.00$ Å with much lower intensities could be also observed. The cross section of the disks in Col_r arrangement can be circular or elliptical projected when the disks are perpendicularly stacked or tilted to the columnar axis. Two columnar Col_r phases, *c2mm* and *p2gg* groups, were commonly identified depending on the point symmetry of the molecules. In compounds **1**, a point symmetry of *c2mm* group was observed since all reflections were matched to $h + k = 2n$ (i.e., the sum equal to an even number[10b]). A model for the formation of columnar phases[2a,3b,4b,10] has been proposed.

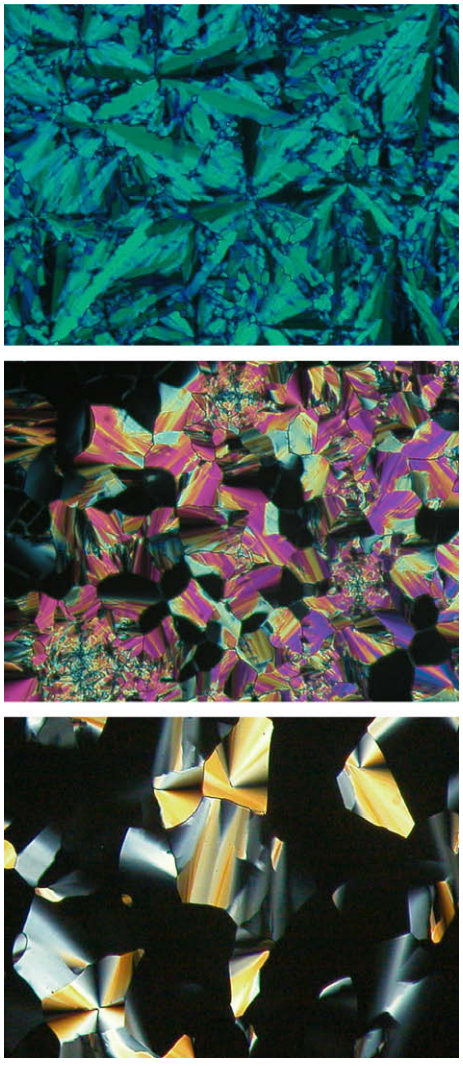

Figure 1. The optical textures (magnification × 100) observed under POM upon the cooling cycle. Top plate: Col_r phase at 95.0 °C of **1** (n = 10), middle plate: Col_h phase at 44.0 °C of **2** (n = 12), and bottom plate: Col_h phase at 40.0 °C of **3** (n = 12).

The phase behavior of the compounds **1**–**4** is summarized in Table 1. The DSC analysis showed a typical columnar phase transition, crystal-to-columnar-to-isotropic (Cr→Col→I). All compounds **1** (except for shorter derivative, n = 8) and **2** exhibited an enantiotropic behavior. All compounds **1** exhibited rectangular columnar phases (Col_r), in contrast, compound **2** formed hexagonal columnar phase (Col_h). For the compounds **1**, the melting temperatures increased with carbon chain length (T_{mp} = −1.60→44.8 °C), however, the clearing temperatures decreased with carbon chain length (T_{cl} = 111.7→84.9 °C). On the other hand, the temperature range of columnar phase was decreasing with carbon chain length, that is, ΔT = 110.1 °C (n = 10) > ΔT = 40.1 °C (n = 16). In addition, a relatively large enthalpy (ΔH = 11.0–17.7 kJ/mol on heating cycle) for the Col_r→I transition was observed, indicating that the molecular order in the columnar phase was relatively high.

On the other hand, a Col_h phase was observed in compound **2** (n = 12). The clearing temperature and transition enthalpy for compound **2** (n = 12) were both dramatically lower than those in compounds **1** (n = 12) by *ca.* ΔT_{cl} = 49.0 °C and ΔH = 10.48 kJ/mol. A lowering in both values indicated a much weaker intermolecular interaction existent in compound **2**. Compound **1** (n = 12) has a wider temperature range than that in compound **2** (n = 12), that is, ΔT_{col} = 89.2 ≫ 2.0 °C. Compound **2** (n = 12) displayed an optical texture of pseudo focal-conics with linear birefringent defects (Fig. 1b), suggesting hexagonal columnar structures. A large area of homeotropic domains was observed, leading to the conclusion of preferred uniaxial character in such Col_h phase. A variable temperature powder XRD experiment confirmed the Col_h phase formed by compound **2** (see Table 2). A diffraction pattern of a hexagonal lattice (Fig. 2) of an intense peak at d 29.13 Å at 46 °C was displayed, which corresponded to Miller indice 1 0 0. This reflection pattern corresponds to an inter-columnar distance (a parameter of the hexagonal lattice) of 33.64 Å. The pseudo-hexagonal lattice constant, that is, a rectangular lattice with an axial ratio of a/b from

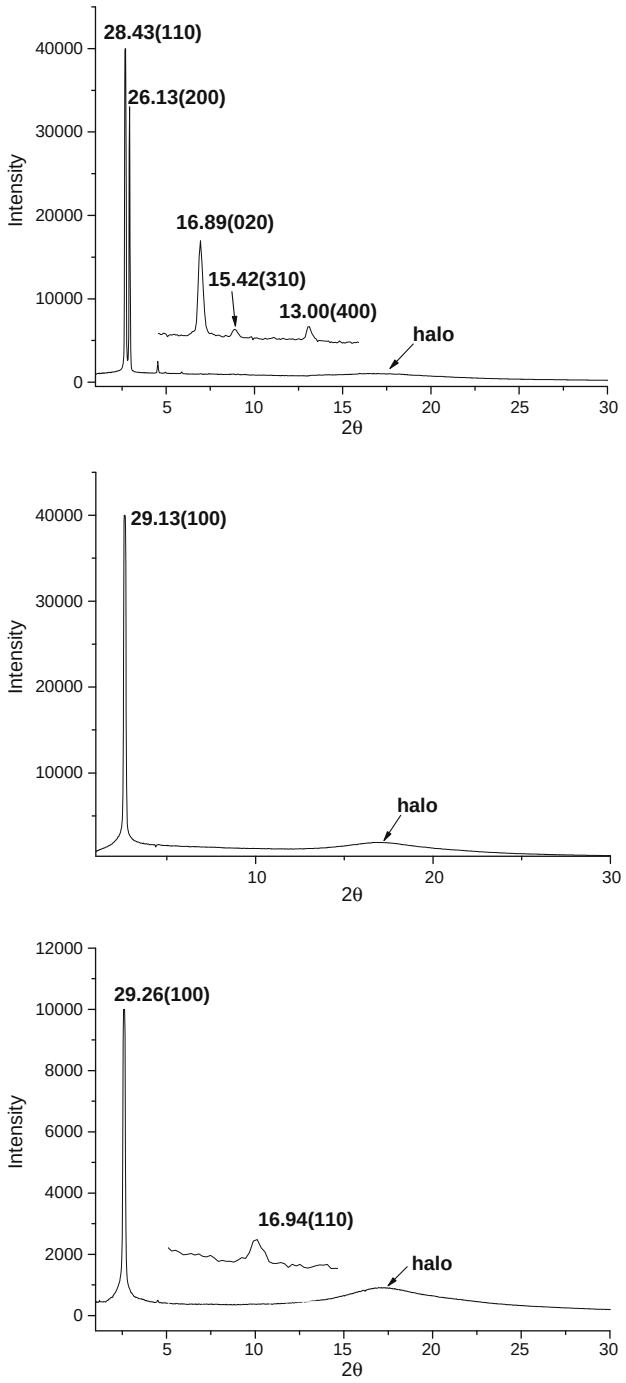

Figure 2. The powder XRD diffraction patterns. Top plot: **1** (n = 12) measured at 77.0 °C, middle plot: **2** (n = 12) measured at 46 °C, and bottom plot: **3** (n = 12) measured at 30.0 °C.

the ideal hexagonal of $3^{1/2}$ a for compound **1** was ranged in 1.91 (n = 10)–1.54 (n = 12), and this value indicated that the structural departure from the ideal hexagonal lattice was about 15–19% in this system. A mesophase[10] that changed from Col_r to Col_h has been observed in other systems, which was generally attributed to the smaller core interaction necessary for the formation of the Col_h phases. The tilted Col_r phase reduced the interactions between the bulky side chains and allowed closer contacts between the cores. A larger atomic size of sulfur atom over oxygen atom was more polarized and a mesophase easily induced, leading to an improved mesophase. A proposed model for molecular arrangements in such columnar phases was shown in Figure 3.

Table 1
The phase transitions and temperatures[a] of compounds **1**–**4**

1	n = 8		Cr ⇌ 118.7 (10.1) / 105.7 (12.3) I
	10	Cr ⇌ -1.60 (17.0) / -4.40 (16.6)	Col_r ⇌ 111.7 (17.7) / 98.3 (16.6) I
	12	Cr ⇌ 13.5 (62.0) / -1.40 (57.0)	Col_r ⇌ 102.7 (15.9) / 86.3 (13.5) I
	14	Cr ⇌ 29.0 (91.5) / 20.4 (86.1)	Col_r ⇌ 90.4 (13.5) / 72.7 (13.9) I
	16	Cr ⇌ 44.8 (87.2) / 40.9 (84.7)	Col_r ⇌ 84.9 (11.0) / 55.0 (8.09) I
2	12	Cr ⇌ 51.7 (76.9) / 42.4 (8.11)	Col_h ⇌ 53.7 (5.42) / 45.9 (7.20) I
3	10		Col_h ⇌ 52.6 (5.71) / 48.4 (5.68) I
	12	Cr ⇌ 16.4 (20.0) / 4.60 (19.9)	Col_h ⇌ 49.8 (6.32) / 46.7 (5.93) I
	14	Cr ⇌ 52.3 (54.0) / 32.2 (54.9)	Col_h ⇌ 53.4 (1.15) / 50.6 (7.03) I
	16		Cr ⇌ 84.2 (13.8) / 48.0 (16.5) I
4	8		Cr ⇌ 67.6 (38.5) / 55.0[b] I
	12		Cr ⇌ 71.0[b] / 65.0[b] I
	16		Cr ⇌ 50.5 (3.90) / 33.7 (50.3) I

[a] n = the carbon numbers of terminal alkoxy chains; Cr = crystal; Col_r = rectangular columnar, Col_h = hexagonal columnar; I = isotropic phases.
[b] Determined by optical microscope.

To understand the effect of heteroatom position incorporated in core structure, compounds **3** were prepared. Both compounds **2** and **3** are structurally similar. Two N atoms and O atoms in compounds **2** are incorporated in *para*-position, however, they are in *meta*-position in compounds **3**. Interestingly, the compounds **3** formed same Col_h phases as compound **2**. Both clearing and melting temperatures of **3** (n = 12) were lower than those in compound **2** (n = 12) by ΔT_{cl} = 3.9 °C and ΔT_{mp} = 35.3 °C, respectively. In contrast, the temperature range of the columnar phase in

Table 2
Detailed indexation at a given temperature of columnar phases for compounds **1**–**3**

Compound	Mesophase	*d*-Spacing (Å) obsd (calcd)	Lattice const.	Miller indices	*a*/*b*
1 (*n* = 10)	Col_r *c2mm* at 75.0 °C	27.02 (27.02)	a_r = 54.04	200	1.91
		25.07 (25.07)	b_r = 28.30	110	
		15.15 (15.20)		310	
		14.19 (14.15)		020	
		13.47 (13.51)		400	
		12.52 (12.54)		220	
		5.57		h	
		4.55		Halo	
1 (*n* = 12)	Col_r *c2mm* at 77.0 °C	28.43 (28.43)	a_r = 52.26	110	1.54
		26.13 (26.13)	b_r = 33.88	200	
		16.89 (16.94)		020	
		15.42 (15.49)		310	
		13.00 (13.07)		400	
		5.61		h	
		4.56		Halo	
1 (*n* = 14)	Col_r *c2mm* at 63.0 °C	29.92 (29.92)	a_r = 55.56	110	1.57
		27.78 (27.78)	b_r = 35.50	200	
		17.69 (17.75)		020	
		16.39 (16.42)		310	
		13.88 (13.89)		400	
		5.57		h	
		4.55		Halo	
1 (*n* = 16)	Col_r *c2mm* at 47.0 °C	31.60 (31.60)	a_r = 59.28	110	1.59
		29.64 (29.64)	b_r = 37.34	200	
		18.56 (18.67)		020	
		17.42 (17.47)		310	
		15.74 (15.80)		220	
		14.77 (14.82)		400	
		5.67		h	
		4.54		Halo	
2 (*n* = 12)	Col_h *p6mm* at 45.0 °C	29.13 (29.13)	a_h = 33.64	100	1.73
		4.53		Halo	
3 (*n* = 10)	Col_h *p6mm* at 50.0 °C	27.14 (17.14)	a_h = 31.34	100	1.73
		4.48		Halo	
3 (*n* = 12)	Col_h *p6mm* at 30.0 °C	29.27 (29.27)	a_h = 33.80	100	1.73
		16.94 (16.90)		110	
		4.43		Halo	
3 (*n* = 14)	Col_h *p6mm* at 50.0 °C	30.71 (30.71)	a_h = 35.46	100	1.73
		17.64 (17.73)		110	
		4.54		Halo	

compounds **3** was much wider than that in compound **2**. The improved mesomorphic behavior observed in compounds **3** was

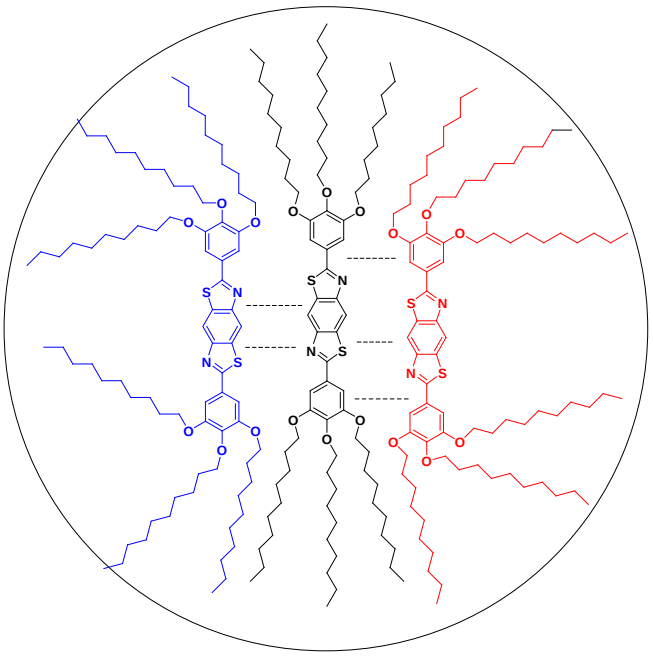

Figure 3. Schematic representing molecular arrangements of hexacatenar mesogens proposed in the hexagonal columnar phase.

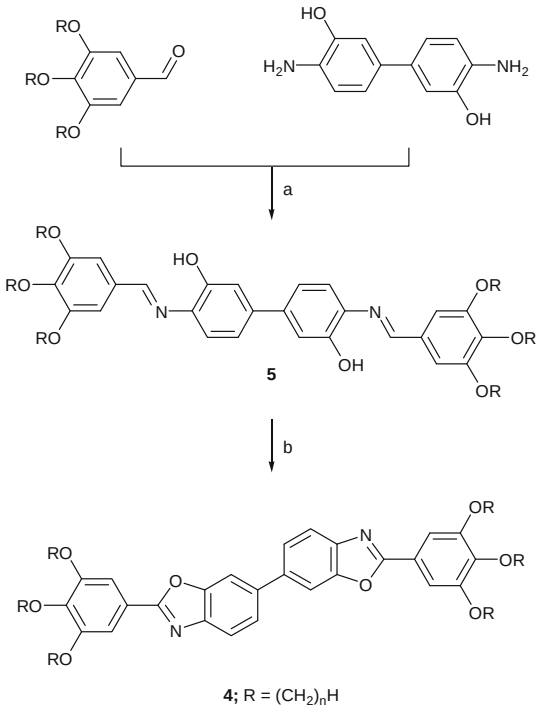

Scheme 2. Reagents and conditions. (a) 3,3′-Dihydroxybenzidine (0.5 equiv), CH_3COOH (drops), refluxed in absolute C_2H_5OH, 6 h, 71–98%; (b) $Pb(OAc)_4$ (2.2 equiv), refluxed in dry CH_2Cl_2, 2 h, 90–96%.

probably attributed to the larger intermolecular dipole–dipole interactions than that in compound **2**. Density functional theory calculations[11] at B3LYP/6-31G(d,p) theoretical level showed that the optimized structures[12] of compounds **2** and **3** have a dipole moment of 3.88 and 6.06 D, respectively. The two electronegative N and O atoms incorporated in *trans*-position of compounds **2** might have a cancellation of the two central dipoles leading to a smaller net dipole moment. In contrast, the position effect of the

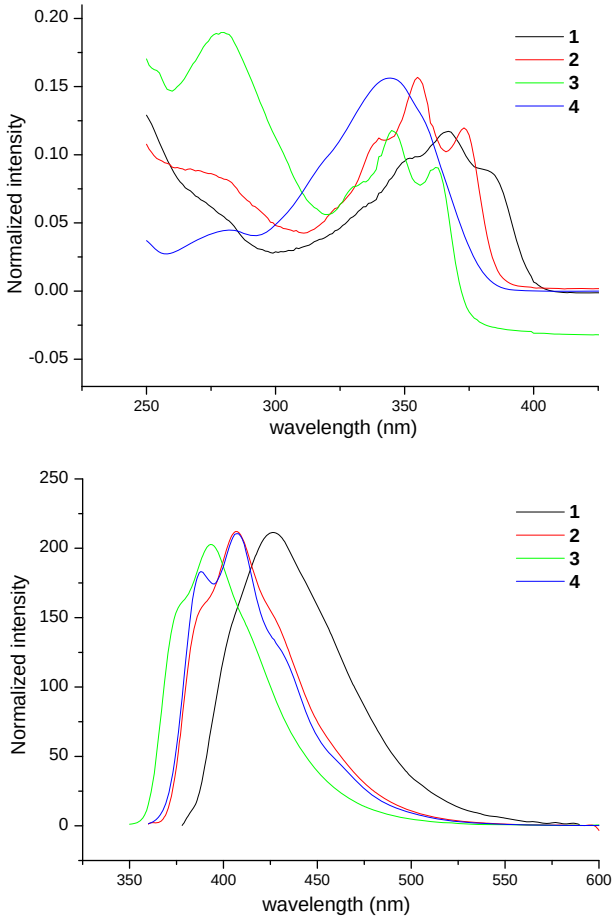

Figure 4. Normalized UV absorption and PL spectra of compounds **1–4** in CH_2Cl_2.

two electronegative N and O atoms in compound **3** might have an addition of the two central dipoles resulting in a larger net dipole moment.

A series of structurally similar compounds **4** (n = 8, 12, 16) were also studied (see Scheme 2), however, they were all non-mesogenic. A phase transition of crystal-to-isotropic at T_{cl} = 67.6 (n = 8) ~50.5 °C (n = 16) was observed. The lack of mesomorphism might be twofold. A longer molecular aspect ratio (d/l) resulted by an extended conjugated core was not favored to the formation of columnar phase. In addition, a density functional theory calculation at B3LYP/6-31G(d,p) theoretical level showed that the optimized structure[12] of compounds **4** (the saturated alkyl chains were modeled by methyl groups.) has a twisted dihedral angle of 38° between the two heterocyclic rings. The non-planar geometry of compounds **4** might not facilitate to the molecular packings in the liquid crystal state.

Heterocyclic derivatives have been an excellent candidate as potential light emitting materials due to their photophysical and fluorescent properties. The luminescent properties observed by such molecules were often affected by substituent and/or conjugation length. The UV–vis absorption and the photoluminescence spectra of the compounds **1-4** (all n's = 12) in CH_2Cl_2 (M = 10^{-5}–10^{-6}) solution are given in Figure 4. The highest absorption peaks of all compounds were found to be insensitive to the carbon length. On the other hand, a similar trend was also observed in the UV–vis absorption/photoluminescence spectra. The λ^{abs} occurred at 344.0–367.0 nm, and the λ^{em} occurred at 394.0–430 nm for compounds **1–4**. Compound **1** (λ^{abs} = 367, λ^{em} = 430 nm) has both spectra slightly red-shift than those of compound **2** (λ^{max} = 355, λ^{em} = 407 nm) due to the larger size and more polarized sulfur atom. On the other hand, a substitution of sulfur atom over oxygen atom in core structure **1** often led to a red shift, due the higher polarizability and basicity of sulfur relative to oxygen. The compound **4** (λ^{max} = 344, λ^{em} = 407 nm) has both spectra blue shifted due to the conjugated length interrupted by two non-coplanar biphenyl rings. However, the quantum yields measured in CH_2Cl_2 estimated with anthracene as a standard (φ_f = 0.27 in hexane) were ranged from 30.1% to 67.4%.

Acknowledgment

This work was supported by the National Science Council of Taiwan, ROC (NSC-96-2113-M-008-003-MY2, NSC-96-2113-M-008-006-MY2 & NSC-95-2752-M-008-010-PAE).

Supplementary data

Supplementary data (synthetic procedures and characterization data for all new compounds **1–4**) associated with this article can be found, in the online version, at doi:10.1016/j.tetlet.2009.02.078.

References and notes

1. (a) He, C. F.; Richards, G. R.; Kelly, S. M.; Contoret, A. E. A.; O'Neill, M. *Liq. Cryst.* **2007**, *34*, 1249–1267; (b) Sultana, N. H.; Kelly, S. M.; Mansoor, B.; O'Neill, M. *Liq. Cryst.* **2007**, *34*, 1307–1316; (c) Huck, D. C.; Nguyen, H. L.; Horton, P. N.; Hursthouse, M. B.; Guillon, D.; Donnio, B.; Bruce, D. W. *Polyhedron* **2006**, *25*, 307–324; (d) Smirnova, A. I.; Bruce, D. W. *J. Mater. Chem.* **2006**, *16*, 4299–4306; (e) Gorecka, E.; Pociecha, D.; Mieczkowski, J.; Matraszek, J.; Donnio, B.; Guillon, D. *J. Am. Chem. Soc.* **2004**, *126*, 15946–15947; (f) Tschierske, C. *Angew Chem., Int. Ed.* **2000**, *39*, 2454–2458; (g) Gorecka, E.; Pociecha, D.; Matraszek, J.; Mieczkowski, J.; Shimbo, Y.; Takanishi, Y.; Takezoe, H. *Phys. Rev.* **2006**, *73*, 31704–31708; (h) Barbera, J.; Cavero, E.; Lehmann, M.; Serrano, J. L.; Sierra, T.; Vázquez, J. T. *J. Am. Chem. Soc.* **2003**, *125*, 4527–4533.
2. (a) Date, R. W.; Iglesias, E. F.; Rowe, K. E.; Elliott, J. M.; Bruce, D. W. *Dalton Trans.* **2003**, 1914–1931; (b) Malthête, J.; Nguyen, H. T.; Destrade, C. *Liq. Cryst.* **1993**, *13*, 171–187; (c) Nguyen, H. T.; Destrade, C.; Malthête, J. *Adv. Mater.* **1997**, *9*, 375–388.
3. (a) Rowe, K. R.; Bruce, D. W. *J. Mater. Chem.* **1998**, *8*, 331–341; (b) Donnio, B.; Heinrich, B.; Gulik-Krzywicki, T.; Delacroix, H.; Guillon, D.; Bruce, D. W. *Chem. Mater.* **1997**, *9*, 2951–2965.
4. (a) Guillon, D.; Heinrich, B.; Ribeiro, A. C.; Cruz, C.; Nguyen, H. T. *Mol. Cryst. Liq. Cryst.* **1998**, *317*, 51–64; (b) Fazio, D.; Mongin, C.; Donnio, B.; Galerne, Y.; Guillon, D.; Bruce, D. W. *J. Mater. Chem.* **2001**, *11*, 2852–2863.
5. Seo, S. H.; Tew, G. N.; Chang, J. Y. *Soft Mater.* **2006**, *2*, 886–891.
6. (a) Shimizu, Y.; Oikawa, K.; Nakayama, K. I.; Guillon, D. *J. Mater. Chem.* **2007**, *17*, 4223–4229; (b) Adam, D.; Schuhmacher, P.; Simmerer, J.; Haussling, L.; Siemensmeyer, K.; Etzbach, K. H.; Ringsdorf, H.; Haarer, D. *Nature* **1994**, *371*, 141–143; (c) van de Craats, A. M.; Warman, J. M. *Adv. Mater.* **2001**, *13*, 130–133; (d) Lemaur, V.; Da Silva Filho, D. A.; Coropceanu, V.; Lehmann, M.; Geerts, Y.; Piris, J.; Debije, M. G.; Van de Craats, A. M.; Senthilkumar, K.; Siebbeles, L. D. A.; Warman, J. M.; Bredas, J. L.; Cornil, J. *J. Am. Chem. Soc.* **2004**, *126*, 3271–3279; (e) van de Craats, A. M.; Stutzmann, N.; Bunk, O.; Nielsen, M. M.; Watson, M.; Mullen, K.; Chanzy, H. D.; Sirringhaus, H.; Friend, R. H. *Adv. Mater.* **2003**, *15*, 495–499; (f) Minch, B. A.; Xia, W.; Donley, C. L.; Hernandez, R. M.; Carter, C.; Carducci, M. D.; Dawson, A.; O'Brien, D. F.; Armstrong, N. R. *Chem. Mater.* **2005**, *17*, 1618–1627; (g) O'Neill, M.; Kelly, S. M. *Adv. Mater.* **2003**, *15*, 1135–1146.
7. (a) Elliott, J. M.; Chipperfield, J. R.; Clark, S.; Sinn, E. *Inorg. Chem. Commun.* **2002**, *5*, 99–101; (b) Rowe, K. E.; Bruce, D. W. *J. Chem. Soc., Dalton Trans.* **1996**, 3913–3915; (c) Bruce, D. W. *Adv. Mater.* **1994**, *6*, 699–701.
8. (a) Alam, M. M.; Jenekhe, S. A. *Chem. Mater.* **2002**, *14*, 4775–4780; (b) Osaheni, J. A.; Jenekhe, S. A. *Chem. Mater.* **1992**, *4*, 1282–1290; (c) Osaheni, J. A.; Jenekhe, S. A. *Macromolecules* **1993**, *26*, 4726–4728; (d) Jenekhe, S. A.; Osaheni, J. A. *Science* **1994**, *265*, 765–768; (e) Osaheni, J. A.; Jenekhe, S. A. *Macromolecules* **1994**, *27*, 739–742.
9. Barche, J.; Janietz, S.; Ahles, M.; Schmechel, R.; Seggern, H. V. *Chem. Mater.* **2004**, *16*, 4286–4291.
10. (a) Donnio, B.; Heinrich, B.; Allouchi, H.; Kain, J.; Diele, S.; Guillon, D.; Bruce, D. W. *J. Am. Chem. Soc.* **2004**, *126*, 15258–15268; (b) Morale, F.; Date, R. W.; Guillon, D.; Bruce, D. W.; Finn, R. L.; Wilson, C.; Blake, A. J.; SchrÖder, M.; Donnio, B. *Chem. Eur. J.* **2003**, *9*, 2484–2501.
11. Density functional theory calculations in this work were performed within the suite of GAUSSIAN 03 programs: Frisch, M. J. et al., GAUSSIAN 03, Revision D.02, Gaussian Inc.: Wallingford, CT, 2004.
12. The saturated alkyl chains were modeled by methyl groups. The optimized structures and direction of dipole are shown in Supplementary data.